AIAA JOURNAL
Vol. 45, No. 11, November 2007

Vibrations of Damaged Cantilevered Beams Manufactured from Functionally Graded Materials

Victor Birman*
University of Missouri–Rolla, St. Louis, Missouri 63121
and
Larry W. Byrd†
U.S. Air Force Research Laboratory, Wright–Patterson Air Force Base, Ohio 45433

DOI: 10.2514/1.30076

This paper is concerned with the effect of damage on free and forced vibrations of a functionally graded cantilever beam. The modes of damage considered in the paper include a region with degraded stiffness adjacent to the root of the beam, a single delamination crack, and a single crack at the root cross section of the beam propagating in the thickness direction. Closed-form solutions are suggested for all cases considered, including both forced and free vibrations; in the case of free vibrations, these solutions are exact. The peculiarities of the frequency analysis of nonprismatic and/or axially graded beams with the root crack in the presence of static thermal loads are also discussed and it is shown that neglecting axial inertia may lead to a qualitative error (this conclusion remains valid in prismatic functionally graded material beams). Numerical examples concentrate on the effect of a single root crack on the fundamental frequency, because such damage was observed in numerous loading scenarios. It is shown that the presence of a crack that has propagated through about one-third of the thickness of the beam significantly affects the fundamental frequency.

Nomenclature

A = extensional stiffness
A_{55} = extensional stiffness in the expression for transverse shear stress resultant
B = coupling stiffness
b = width of the beam
D = bending stiffness
d = depth of the crack
f = fundamental frequency
K = rotational stiffness of the support
k = nondimensional compliance
$\tilde{k}^2$ = shear correction factor
M = stress couple (beam of the rectangular cross section) or bending moment (arbitrary cross section)
m = mass per unit surface area (beam of the rectangular cross section) or mass per unit length (arbitrary cross section)
N = stress resultant (beam of the rectangular cross section) or axial force (arbitrary cross section)
P = static force
T = Temperature
t = Time
Q = transverse shear stress resultant (beam of the rectangular cross section) or transverse shear force (arbitrary cross section)
Q_{11} = reduced stiffness
q = dynamic magnification factor
u = axial displacement
v = kinematic excitation (motion of the support)
w = transverse deflection
x = axial coordinate
y = coordinate in the width direction of the beam
z = transverse coordinate
α = coefficient of thermal expansion
δ = displacement of the tip of a cantilever beam
φ = normal mode (axial motion)
η = normal mode
λ = natural frequency
ρ = local value of the mass density of the functionally graded material
ω = driving frequency
ψ = rotation of an element that was perpendicular to the beam axis before deformation

I. Introduction

FUNCTIONALLY graded materials (FGMs) have attracted the considerable attention of researchers and engineers due to a number of attractive features, such as a reduction or elimination of the interfacial stresses that often cause delamination in layered composites and enhanced thermal properties. A number of reviews dealing with various aspects of FGM have been published in recent years [1–4].

Previous research on FGM beams includes the paper by Sankar [5], who considered a FGM beam subjected to a sinusoidal transverse load applied at one of the surfaces. The problems of free vibrations, wave propagation, and static deformations in FGM shear deformable beams were solved in [6,7] using a specially developed finite element accounting for the power law and other alternative variations of elastic and thermal properties in the thickness direction.

Extensive work on the development of functionally graded piezoelectric actuators dealing with various aspects of manufacturing, modeling, and design of piezoelectric FGM beams has been conducted during the last decade. The effect of the grading of one of the critical properties such as conductivity, piezoelectric coefficient, permittivity, or porosity is considered in [8–11]. A new class of piezoceramic functionally graded actuators using the so-called dual-electro/piezo-property gradient technique that emphasizes variations of both piezoelectric coefficients and the electric permittivity was considered in [12].

Contrary to the cited papers concentrating on intact beams, the present solutions address the problems of free and forced vibrations of cantilever FGM beams with various modes of damage, including cracks propagating perpendicular to the beam surface and

Received 28 January 2007; revision received 1 April 2007; accepted for publication 2 April 2007.

*Engineering Education Center, One University Boulevard. Associate Fellow AIAA.
†Analytical Structural Mechanics Branch, Structural Sciences Center.

delamination cracks. A particular mode of damage found in a beam depends on the nature of applied loading. For example, a single through-the-thickness crack in the vicinity of the root of the beam is anticipated in cases in which the load is either static or harmonic in time and the maximum bending moment is at the root. However, an impact may result in a continuous region with degraded stiffness, as well as in delamination cracks in layered beams. Numerical analysis is presented in the paper for a single through-the-thickness crack adjacent to the root of the beam.

FGM beams often operate in high-temperature environments. For example, a FGM turbine blade can be modeled as a nonprismatic cantilever beam subject to temperature predominantly varying in the thickness direction. The paper elucidates the factors that should be considered in the free-vibration analysis of nonprismatic FGM beams with a root crack (this illustration is also applicable to FGM beams with axially variable grading). It is shown that some aspects of the thermal effect on the natural frequencies will be disregarded if one neglects the contribution of axial inertia.

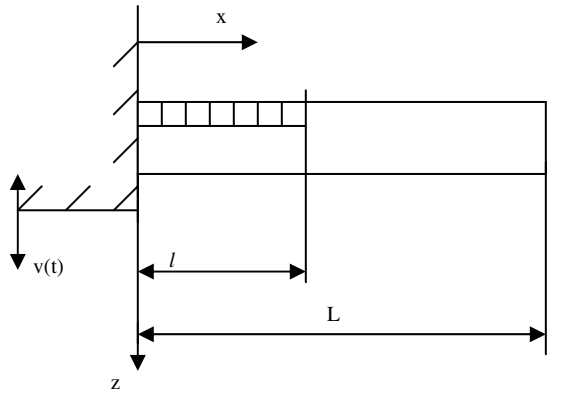

Fig. 1 A cantilever beam with the region of degraded stiffness; the beam is subdivided into region 1 (intact part of the beam, $l \le x \le L$) and region 2 (part of the beam with degraded stiffness, $0 \le x \le l$).

II. Analysis

Consider forced vibrations of a cantilever FGM beam driven by the motion of its support that is a harmonic function of time (i.e., $v = V \sin \omega t$). A typical mode of damage in FGM cantilever beams is represented by cracks oriented in the direction that is perpendicular to the beam surface and concentrated in the immediate vicinity to the clamped end (Fig. 1). Delamination cracks may also develop in layered FGM cantilever beams with layerwise constant volume fractions of constituent phases (Fig. 2). A single crack is often observed in laminated beams and in particulate FGM beams (Fig. 3).

The analysis is conducted by assumption that the amplitude of motion remains small (i.e., a geometrically linear theory is applicable). Transverse shear deformations can be omitted if the beams and the regions of the beams considered in the analysis have a length-to-thickness ratio of no less than 20. However, for shorter beam regions, a first-order shear deformation theory (FSDT) should be applied, providing accurate predictions for eigenvalues such as buckling loads [13] and natural frequencies. The material of the beam is assumed to remain within the elastic range in all cases considered next.

For the problems that can be considered by a technical (slender) beam theory, the axial stress resultant and the bending stress couple are given by

$$N = A\frac{\partial u}{\partial x} - B\frac{\partial^2 w}{\partial x^2}, \qquad M = B\frac{\partial u}{\partial x} - D\frac{\partial^2 w}{\partial x^2} \tag{1}$$

where the stiffness terms are defined by standard equations. The following solution can be extended to a more general case in which the cross section of the beam is not rectangular. However, in such a case, N and M are the axial force and bending moment, respectively, and the stiffness terms can be found from

$$\{A, B, D\} = \int_y \int_z E_x(y, z)\{1, z, z^2\}\, \mathrm{d}z\, \mathrm{d}y \tag{2}$$

where E_x is the local modulus in the axial direction or the corresponding reduced stiffness. The integration in Eq. (2) should be performed over the thickness and width of the beam. Note that the definition of the stiffness terms (2) implies that the analysis using these terms is applicable to an arbitrary FGM, including materials with a continuous variation of volume fractions of the constituent phases and stepwise layered particulate composites. The local modulus of elasticity can be determined by a homogenization method applicable to FGM with an arbitrary distribution of constituent phases through the thickness, such as the Mori–Tanaka method or the self-consistent method.

In the case in which it is necessary to specify the transverse shear stress resultant or force in the absence of applied axial loads and to neglect geometrically nonlinear effects, it can be determined from the equilibrium equation $Q = \partial M/\partial x$.

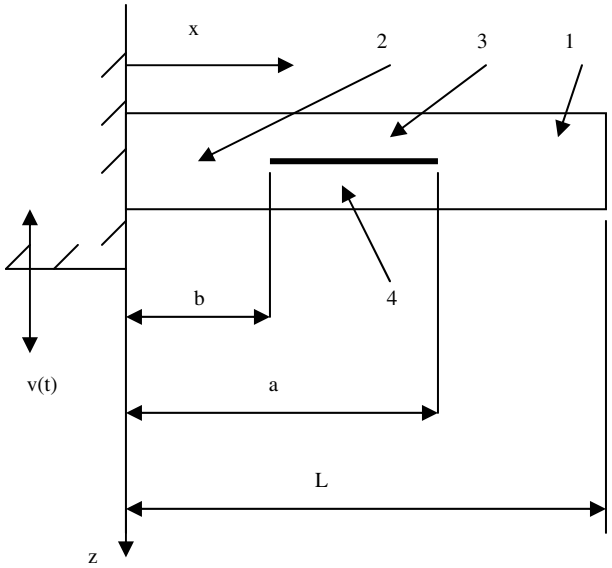

Fig. 2 A cantilever beam with a delamination crack; regions 1–4 are referred to in the analysis.

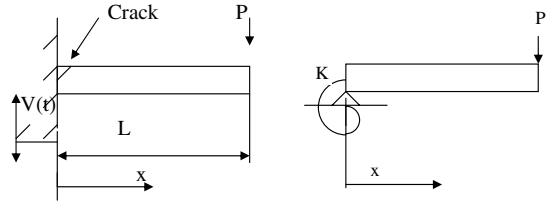

Fig. 3 A cantilever beam with a single crack in the vicinity of the support modeled as a beam with a rotational spring: the actual beam with a root crack (left) and the model used in the analysis (right); static force P is used to determine the spring constant (coefficient K).

A. Slender Beam with a Degraded Stiffness Region Modeled by the Bernoulli–Euler Theory

Consider a beam of rectangular cross section (shown in Fig. 1) that has a region of degraded stiffness. The solution of the vibration problem is possible if the beam is subdivided into two regions of different stiffness, as shown in Fig. 1. The equations of free vibrations for each region of the beam, written by assumption that the slender beam theory is applicable, are

$$A_n \frac{\partial u_n^2}{\partial x^2} - B_n \frac{\partial^3 w_n}{\partial x^3} - m_n \ddot{u}_n = 0 \tag{3a}$$

$$B_n \frac{\partial^3 u_n}{\partial x^3} - D_n \frac{\partial^4 w_n}{\partial x^4} - m_n(\ddot{w}_n + \ddot{v}) = 0 \tag{3b}$$

where $n = 1, 2$ is a number of the region and the transverse deflection w is counted relative to the moving support.

The solution must satisfy the boundary and continuity conditions:

$$\begin{aligned} &x = 0\text{: } w_2 = 0, \qquad \frac{\mathrm{d}w_2}{\mathrm{d}x} = 0 \\ &x = L\text{: } M_1 = 0, \qquad Q_1 = 0 \\ &x = l\text{: } w_1 = w_2, \qquad \frac{\mathrm{d}w_1}{\mathrm{d}x} = \frac{\mathrm{d}w_2}{\mathrm{d}x} \\ &\qquad M_1 = M_2, \qquad Q_1 = Q_2 \end{aligned} \tag{4}$$

Additionally, axial displacements and stress resultants should satisfy the following requirements:

$$\begin{aligned} &x = 0\text{: } u_2 = 0 \\ &x = l\text{: } u_1 = u_2, \qquad N_1 = N_2 \\ &x = L\text{: } N_1 = 0 \end{aligned} \tag{5}$$

The first condition of Eq. (5) may become questionable if the damage propagates through more than a half-thickness of the beam. However, such cases correspond to an excessive degree of damage that is not considered here.

Notably, it is impossible to analyze vibrations of a cantilever beam while neglecting the axial inertia altogether. It is easily observed that such simplification combined with the continuity requirement for the axial stress resultants would imply the absence of the axial force at the clamped end of the beam. However, such a boundary condition for the axial force contradicts the first condition of Eq. (5).

Two approaches to the solution of the problem could be considered. The more accurate, though time-consuming, method could be developed along the lines of the solution shown for shear deformable FGM beams in Sec. II.B. The solution illustrated in the present section is simpler, relying on the assumption that although the axial inertia affects the dynamic equilibrium in the corresponding direction [Eq. (3a)], its effect on the transverse equilibrium can be neglected. This is justified by the observation that a slender beam has a much larger stiffness in the spanwise direction when compared with that in the transverse direction. As a result, the effect of the axial inertia on transverse vibrations is negligible. This simplification is further justified by the results shown in Numerical Examples, in which the analytical solution obtained while neglecting the axial inertia is compared with the FEA solution accounting for it. In addition, the effect of the axial inertia on the fundamental frequency of a composite beam is estimated in the Appendix.

In view of numerous studies in which transverse motion of the beams has been accurately evaluated without accounting for the axial inertia, the methodology adopted in this section should produce acceptable results.

In the problem of free vibrations, the motion within each region of the beam can be represented by

$$u_n = U_n(x) \sin \lambda t, \qquad w_n = W_n(x) \sin \lambda t \tag{6}$$

The substitution of Eq. (6) into Eq. (3) and neglecting the axial inertia yields

$$\begin{aligned} W_n = {} & C_1^{(n)} \sinh \beta_n x + C_2^{(n)} \cosh \beta_n x \\ & + C_3^{(n)} \sin \beta_n x + C_4^{(n)} \cos \beta_n x \end{aligned} \tag{7a}$$

$$\beta_n = \sqrt[4]{\frac{m_n \lambda^2}{D_n - (B_n^2/A_n)}} \tag{7b}$$

where $C_j^{(n)}$ are constants of integration. The substitution of Eqs. (6) and (7) into Eq. (3a) and retaining the axial inertia term yields

$$\begin{aligned} U_n = {} & C_5^{(n)} \sin \gamma_n x + C_6^{(n)} \cos \gamma_n x \\ & + B_n \beta_n^3 \left[\frac{C_1^{(n)} \cosh \beta_n x + C_2^{(n)} \sinh \beta_n x}{m_n \lambda^2 + A_n \beta_n^2} \right. \\ & \left. + \frac{C_4^{(n)} \sin \beta_n x - C_3^{(n)} \cos \beta_n x}{m_n \lambda^2 - A_n \beta_n^2} \right] \\ \gamma_n = {} & \lambda \sqrt{\frac{m_n}{A_n}} \end{aligned} \tag{8}$$

Upon the substitution of displacements given by Eqs. (7) and (8), boundary and continuity conditions (4) and (5) yield a system of 12 homogeneous algebraic equations with respect to 12 constants of integration $C_r^{(n)}$ ($r = 1, 2, \ldots, 6$). The nonzero requirement for these constants yields the frequency equation and eigenvectors.

Consider now forced vibrations of a beam driven by the harmonic motion of its support. In this case, the solution can be obtained in terms of normal modes (mode-summation method). For example, the transverse motion can be represented as

$$w = \sum_i W_i \left[\delta(0 \le x \le l) \eta_2^{(i)}(x) + \delta(l < x \le L) \eta_1^{(i)}(x) \right] \sin \omega t \tag{9}$$

where $\delta(x_s \le x \le x_r) = 1$ if $x_s \le x \le x_r$ and zero otherwise, and W_i are unknown amplitudes. The normal modes corresponding to the natural frequency λ_i are

$$\begin{aligned} \eta_n^{(i)}(x) = {} & k_{1ni} \sinh \beta_{ni} x + k_{2ni} \cosh \beta_{ni} x \\ & + k_{3ni} \sin \beta_{ni} x + k_{4ni} \cos \beta_{ni} x \end{aligned} \tag{10}$$

where k_{jni} are the elements of the normalized eigenvector corresponding to the ith eigenvalue, and β_{ni} is obtained from Eq. (7) using $\lambda = \lambda_i$.

The application of the Galerkin method and neglecting the effect of the axial inertia on forced transverse vibrations yield uncoupled equations for the amplitudes of the corresponding terms in Eq. (9):

$$\begin{aligned} & W_i \left\{ \int_0^l \left[\left(D_2 - \frac{B_2^2}{A_2} \right) \beta_{2i}^4(\lambda_i) \eta_2^{(i)} - m\omega^2 \eta_2^{(i)} \right] \eta_2^{(i)} \, \mathrm{d}x \right. \\ & \left. + \int_l^L \left[\left(D_1 - \frac{B_1^2}{A_1} \right) \beta_{1i}^4(\lambda_i) \eta_1^{(i)} - m\omega^2 \eta_1^{(i)} \right] \eta_1^{(i)} \, \mathrm{d}x \right\} \\ & = m\omega^2 V \left[\int_0^l \eta_2^{(i)} \, \mathrm{d}x + \int_l^L \eta_1^{(i)} \, \mathrm{d}x \right] \end{aligned} \tag{11}$$

This equation can be further simplified, yielding

$$\begin{aligned} W_i &= \frac{m\omega^2 V [\int_0^l \eta_2^{(i)} \, \mathrm{d}x + \int_l^L \eta_1^{(i)} \, \mathrm{d}x]}{M_i(\lambda_i^2 - \omega^2)} \\ M_i &= m \left[\int_0^l \left(\eta_2^{(i)} \right)^2 \mathrm{d}x + \int_l^L \left(\eta_1^{(i)} \right)^2 \mathrm{d}x \right] \end{aligned} \tag{12}$$

B. Natural Frequencies of a FGM Beam with a Region of Reduced Stiffness

Although a typical FGM beam in potential applications is slender, the region with damage (region 2 in Fig. 1) may be relatively short. In this case, such a region should be analyzed, accounting for transverse shear effects. Accordingly, this section illustrates an exact solution for the natural frequencies of FGM cantilever beams by the FSDT. Both regions 1 and 2 are analyzed by this theory for consistency, even though the intact region may be slender.

The expressions for the axial and transverse shear stress resultants and for the bending stress couple according to FSDT are [14,15]

$$N = A\frac{\partial u}{\partial x} + B\frac{\partial \psi}{\partial x}, \qquad M = B\frac{\partial u}{\partial x} + D\frac{\partial \psi}{\partial x}$$
$$Q = \tilde{k}^2 A_{55}\left(\psi + \frac{\partial w}{\partial x}\right) \tag{13}$$

It is noted that the shear correction factor k in Eq. (13) is affected by a distribution of the stiffness throughout the thickness of the beam. It is possible to evaluate this factor using the approach proposed by Bert and Gordaninejad [16] that was developed using a comparison between the shear strain energy of the actual beam with the energy for an equivalent Timoshenko beam. This solution provides the value of the shear correction factor as a function of the integrals affected by the variations of the modulus of elasticity and the Poisson ratio throughout the thickness.

Equations of motion of a unit-width beam, accounting for axial, rotational, and transverse inertias, are [14,15]

$$A\frac{\partial^2 u}{\partial x^2} + B\frac{\partial^2 \psi}{\partial x^2} = m\ddot{u} + H\ddot{\psi}$$
$$B\frac{\partial^2 u}{\partial x^2} + D\frac{\partial^2 \psi}{\partial x^2} - kA_{55}\left(\psi + \frac{\partial w}{\partial x}\right) = H\ddot{u} + I\ddot{\psi} \tag{14}$$
$$\tilde{k}^2 A_{55}\left(\frac{\partial \psi}{\partial x} + \frac{\partial^2 w}{\partial x}\right) = m\ddot{w}$$

where

$$\{H, I\} = \int_z \rho(z)\{z, z^2\}\,\mathrm{d}z$$

and the integration is conducted through the thickness of the beam.

In the problem of free vibrations, the motion is assumed to be harmonic and the terms in the right side of Eq. (14) are modified accordingly (i.e., $\{\ddot{u}, \ddot{\psi}, \ddot{w}\} = -\lambda^2\{u, \psi, w\}$). The exact solution of the problem is similar to the approach discussed in the monograph of Reddy [15]. The highest-order derivatives of the displacements and rotation are expressed from Eq. (14):

$$\frac{\partial^2 u}{\partial x^2} = f_1\psi + f_2\frac{\partial \psi}{\partial x} + f_3 w + f_4\frac{\partial w}{\partial x} + f_5 u$$
$$\frac{\partial^2 \psi}{\partial x^2} = f_6\psi + f_7\frac{\partial \psi}{\partial x} + f_8 w + f_9\frac{\partial w}{\partial x} + f_{10} u \tag{15}$$
$$\frac{\partial^2 w}{\partial x^2} = f_{11}\psi + f_{12}\frac{\partial \psi}{\partial x} + f_{13} w + f_{14}\frac{\partial w}{\partial x} + f_{15} u$$

where the expressions for the coefficients $f_{mn} = f_{mn}(\lambda)$ are easily available. Subsequently, the vector of displacements and their derivatives is introduced:

$$\{\bar{R}\} = \{\,\psi \quad \tfrac{\partial \psi}{\partial x} \quad w \quad \tfrac{\partial w}{\partial x} \quad u \quad \tfrac{\partial u}{\partial x}\,\}^T \tag{16}$$

The system of Eqs. (15) is now replaced with

$$\left\{\frac{\partial \bar{R}}{\partial x}\right\} = [T]\{\bar{R}\} \tag{17}$$

The elements of the square matrix T are

$$T_{1j} = 0 \quad (j \neq 2), \quad T_{12} = 1, \quad T_{21} = f_6 \quad T_{22} = f_7,$$
$$T_{23} = f_8, \quad T_{24} = f_9, \quad T_{25} = f_{10} \quad T_{26} = 0, \quad T_{3j} = 0$$
$$(j \neq 4), \quad T_{34} = 1 \quad T_{41} = f_{11}, \quad T_{42} = f_{12},$$
$$T_{43} = f_{13}, \quad T_{44} = f_{14} \quad T_{45} = f_{15}, \quad T_{46} = 0,$$
$$T_{5j} = 0 \quad (j \neq 6) \quad T_{56} = 1, \quad T_{61} = f_1, \quad T_{62} = f_2,$$
$$T_{63} = f_3 \quad T_{64} = f_4, \quad T_{65} = f_5, \quad T_{66} = 0 \tag{18}$$

Following Dorf [17], the solution is sought in the form

$$\{\bar{R}\} = e^{[T]x}\{\bar{K}\} \tag{19}$$

where $\{\bar{K}\}$ is a sixth-order vector of unknown constants and

$$e^{[T]x} = \sum_{r=0} \frac{[T]^r x^r}{r!} \tag{20}$$

It is immediately obvious that Eq. (19) satisfies Eq. (17). Furthermore, Eqs. (19) and (20) can be represented in the form

$$\{\bar{R}_n\} = [P_n(x, \lambda)]\{\bar{K}_n\} \tag{21}$$

where n identifies the beam region. For example, limiting series (20) to $r \leq 3$, the ijth element of the matrix $[P_n(x, \lambda)]$ is

$$P_{ij}^{(n)} = I_{ij} + T_{ij}x + \frac{1}{2}\sum_{k=1}^{6} T_{ik}T_{kj}x^2 + \frac{1}{6}\sum_{s=1}^{6}\sum_{k=1}^{6} T_{is}T_{sk}T_{kj}x^3 \tag{22}$$

where I_{ij} is an element of an identity matrix.

The boundary and continuity conditions that have to be satisfied are

$$x = 0\text{: } w_2 = u_2 = \psi_2 = 0$$
$$x = L\text{: } M_1 = Q_1 = N_1 = 0$$
$$x = l\text{: } w_1 = w_2, \quad u_1 = u_2, \quad \psi_1 = \psi_2$$
$$M_1 = M_2, \quad Q_1 = Q_2, \quad N_1 = N_2 \tag{23}$$

There are 12 conditions that can be represented as a system of homogenous equations with respect to 12 unknown constants of integration:

$$[S(\lambda)]\begin{Bmatrix}\{K_1\}\\ \{K_2\}\end{Bmatrix} = 0 \tag{24}$$

The frequency equation (i.e., $\det[S(\lambda)] = 0$) yields the values of natural frequencies.

C. Beams with a Delamination Crack

Consider the case in which a FGM cantilever beam of a rectangular cross section with a layerwise constant volume fraction of constituent phases has a delamination crack (Fig. 2). The beam can be subdivided into regions, as shown in Fig. 2.

Vibrations of delaminated composite beams have been considered by numerous investigators (see [18] for a review of relevant work published before 2000). The complication involved in the study is related to the necessity to define a contact law between two delaminated regions of the beam during the cycle of motion. It is reasonable to assume that as the distance between regions 3 and 4 increases compared with the static configuration (i.e., the delamination crack becomes wider), the contact pressure between these regions is equal to zero. However, during the other part of the cycle, the distance between regions 3 and 4 decreases and eventually, the crack may close. The contact law during the motion corresponding to a narrowing (but not closed) delamination crack reflects the presence of a partially intact matrix and fibers within the crack. Luo and Hanagud [18] modeled the interaction between regions 3 and 4 by a spring with a linear force-distance relationship within the range of deflections (w_3–w_4) varying from zero to the value corresponding to a closed crack. The spring constant would be determined from experiments. Wang and Tong [19] considered two different contact laws between delaminated regions, including a linear spring and a nonlinear Hertz-type contact function. Contrary to [18], the stiffness of the linear spring was approximated by an effective modulus of two springs in series, each spring reflecting the stiffness of the corresponding region of the beam. A constant in the Hertz-type contact law in which the reaction was proportional to a 1.5 power of the distance between the regions was chosen arbitrarily.

The complexity of the analysis described earlier is related to difficulties associated with specifying the contact law for the part of motion cycle when the regions begin to press against each other. In addition to an uncertain amount of residual material within the crack, its width should also affect the exact distance between the regions when they begin to apply pressure to each other. Noticeably, some studies assume that vibrations of delaminated regions occur with small enough amplitude so that the crack always remains open [20]. In the present paper, we suggest a different approach; that is, instead of trying to exactly define the fundamental frequency of the beam with a delamination or a notch, we establish the boundaries of this frequency. The lower boundary corresponds to the beam in which the regions of the beam vibrate without any contact pressure. The upper boundary is evaluated by assuming that during a part of the cycle when the distance between the regions increases, the pressure between them is equal to zero and that during the other part of the cycle, the regions move toward each other and the crack is closed, so that the beam vibrates as an intact structure. This implies that it is sufficient to determine two frequencies: the lower frequency λ' found from the analysis shown next and the upper frequency $\lambda'' = 2/(\lambda'^{-1} + \tilde{\lambda}^{-1})$, where $\tilde{\lambda}$ is a frequency of the intact structure. The actual natural frequency will be within the range $\lambda' < \lambda < \lambda''$. Accordingly, the present section illustrates the analysis of vibrations of the beam without a contact between delaminated regions that would yield the lower limit for the frequency. Note that as long as the crack remains short and vibrations are linear, it is anticipated that the effect of the pressure between delaminated regions will be small, with the fundamental frequency being close to the lower limit. The issue of closing cracks is also revisited in Sec. II.D.

The free vibrations of each region are characterized by Eqs. (3), in which $v = 0$ as long as the slender beam theory is applicable. Note that the term accounting for the stretching of the beam axis [i.e., $N_n(\partial^2 w_n/\partial x^2)$] does not appear in these equations because it is nonlinear (this term would be present in the linear formulation only if an axial force was applied to the beam). The exception may be found in the case in which residual stresses, though in self-equilibrium at every cross section, vary throughout the depth of the beam. In such a case, the static stress resultants appear in the equations of motion for regions 3 and 4 and the analysis will be affected by the corresponding terms (this situation is not considered here, though the present analysis could be expanded to account for such residual effects).

In the case in which the effect of the axial inertia on the equation of motion in the transverse direction is neglected, Eqs. (7) and (8) represent free vibrations of each of four regions of the beam.

The constants of integration are determined from the boundary conditions at the ends $x = 0$ and $x = L$, as given by Eq. (4) and the axial boundary conditions:

$$u_2(x = 0) = 0, \qquad N_1(x = L) = 0 \tag{25}$$

The continuity conditions for the adjacent regions are formulated by an extrapolation of the solution for delamination buckling problems developed by Simitses [21]:

$$\begin{aligned} &x = a\text{: } w_1 = w_3 = w_4, \qquad \frac{\mathrm{d}w_1}{\mathrm{d}x} = \frac{\mathrm{d}w_3}{\mathrm{d}x} = \frac{\mathrm{d}w_4}{\mathrm{d}x} \\ &\qquad M_1 = M_3 + M_4, \qquad Q_1 = Q_3 + Q_4, \qquad N_3 + N_4 = 0 \\ &x = b\text{: } w_2 = w_3 = w_4, \qquad \frac{\mathrm{d}w_2}{\mathrm{d}x} = \frac{\mathrm{d}w_3}{\mathrm{d}x} = \frac{\mathrm{d}w_4}{\mathrm{d}x} \\ &\qquad M_2 = M_3 + M_4, \qquad Q_2 = Q_3 + Q_4, \qquad N_2 = N_3 + N_4 \end{aligned} \tag{26}$$

In addition to Eq. (26), it is necessary to satisfy the continuity of axial displacements for adjacent regions, that is,

$$\begin{aligned} &x = a\text{: } u_3 = u_1 + z_{13}w_{1,x}, \qquad u_4 = u_1 + z_{14}w_{1,x} \\ &x = b\text{: } u_3 = u_2 + z_{23}w_{2,x}, \qquad u_4 = u_2 + z_{24}w_{2,x} \end{aligned} \tag{27}$$

where $z_{13} = z_{23}$, $z_{14} = z_{24}$ are the distances between the centroids of the corresponding regions of the beam, taken with the appropriate sign according to Fig. 2.

The expressions for W_n and U_n for four regions of the beam contain 24 constants of integration. Substituting these expressions into four boundary conditions (4) that refer to the ends of the beam, two axial boundary conditions (25) and 18 continuity conditions (26) and (27) yields a system of 24 linear homogeneous algebraic equations for the constants of integration. The frequency equation is formulated based on the nonzero requirement to these constants. The eigenvalues (frequencies) and eigenvectors (mode shapes) can be evaluated from this equation.

Forced vibrations of the beam can now be found as an appropriate modification of the previous solution for the case of a region of degraded stiffness. For example, the transverse motion is represented by

$$w = \sum_i W_i[\delta(0 \le x \le b)\eta_2^{(i)}(x) + \delta(a < x \le L)\eta_1^{(i)}(x) + \delta(b \le x \le a, z_3)\eta_3^{(i)}(x) + \delta(b \le x \le a, z_4)\eta_4^{(i)}(x)]\sin\omega t \tag{28}$$

where $\delta(x_1 \le x \le x_2, z_m)$ identifies the corresponding region of the beam ($m = 3, 4$).

The Galerkin equation for W_i obtained by assumption that the contribution of the axial inertia is negligible is

$$\begin{aligned} W_i\Bigg\{&\int_0^b\left[\left(D_2 - \frac{B_2^2}{A_2}\right)\beta_2^4(\lambda_i)\eta_2^{(i)} - m\omega^2\eta_2^{(i)}\right]\eta_2^{(i)}\,\mathrm{d}x \\ &+ \int_a^L\left[\left(D_1 - \frac{B_1^2}{A_1}\right)\beta_1^4(\lambda_i)\eta_1^{(i)} - m\omega^2\eta_1^{(i)}\right]\eta_1^{(i)}\,\mathrm{d}x \\ &+ \int_b^a\left[\left(D_3 - \frac{B_3^2}{A_3}\right)\beta_3^4(\lambda_i)\eta_3^{(i)} - m_3\omega^2\eta_3^{(i)}\right]\eta_3^{(i)}\,\mathrm{d}x \\ &+ \int_b^a\left[\left(D_4 - \frac{B_4^2}{A_4}\right)\beta_4^4(\lambda_i)\eta_4^{(i)} - m_4\omega^2\eta_4^{(i)}\right]\eta_4^{(i)}\,\mathrm{d}x\Bigg\} \\ &= \omega^2 V\left[m\int_0^b \eta_2^{(i)}\,\mathrm{d}x + m\int_a^L \eta_1^{(i)}\,\mathrm{d}x + m_3\int_b^a \eta_3^{(i)}\,\mathrm{d}x + m_4\int_b^a \eta_4^{(i)}\,\mathrm{d}x\right] \end{aligned} \tag{29}$$

where m, m_3, and m_4 refer to the mass per unit surface of the corresponding beam region.

This equation can be further simplified by introducing

$$\begin{aligned} M_i' = &m\int_0^b (\eta_2^{(i)})^2\,\mathrm{d}x + m\int_a^L (\eta_1^{(i)})^2\,\mathrm{d}x \\ &+ m_3\int_b^a (\eta_3^{(i)})^2\,\mathrm{d}x + m_4\int_b^a (\eta_4^{(i)})^2\,\mathrm{d}x \end{aligned} \tag{30}$$

Then the expression for the amplitude of the ith term in Eq. (28) is

$$\begin{aligned} W_i = \frac{\omega^2 V}{M_i'(\lambda_i^2 - \omega^2)}\Bigg[&m\int_0^b \eta_2^{(i)}\,\mathrm{d}x + m\int_a^L \eta_1^{(i)}\,\mathrm{d}x \\ &+ m_3\int_b^a \eta_3^{(i)}\,\mathrm{d}x + m_4\int_b^a \eta_4^{(i)}\,\mathrm{d}x\Bigg] \end{aligned} \tag{31}$$

D. Beams with a Single Crack in the Vicinity of the Support

As was observed in experiments, fracture in an isotropic cantilever beam is often associated with a single crack located close to the support and oriented perpendicular to the beam surface (root crack). In the case of a harmonic dynamic loading, two cracks may start propagating toward each other from the opposite surfaces of the beam. In FGM beams composed of pseudoisotropic layers of particulate materials with a layerwise constant volume fraction of the

constituents, a single crack close to the support is also a likely scenario. The effect of such a crack that practically coincides with a part of the clamped boundary is considered in this section of the paper.

The approach adopted in this paper is based on modeling the effect of the crack through a rotational spring at the clamped end (Fig. 3). This reflects the fact that although the crack does not affect the resistance to transverse deflections at the clamped end, a certain degree of compliance to rotational deformations about this end is unavoidable. Therefore, it is possible to incorporate the effect of the crack, combining experimental or numerical data on the rotational stiffness at the clamped end with the analytical solution. Note that in line with the previous discussion on the effect of the interaction between delaminated regions of a beam during the part of the cycle when the distance between the regions decreases, it is necessary to account for the effect of the closing of the crack during the motion. Accordingly, the present solution refers to the case in which the crack remains open and there is no mechanical pressure between the parts of the beam and support encompassing the crack (lower limit of the fundamental frequency). The upper limit of the solution obtained by assuming that the crack is closed during the part of motion when the beam rotates in the counterclockwise direction (refer to Fig. 3), is estimated in numerical examples. The proposed approach includes three steps outlined next.

1. Static Problem for the Free-End Deflection

Consider a relationship between the deflection of the free end of the FGM beam of a rectangular cross section (shown in Fig. 3) and the coefficient of elastic rotational constraint introduced by the elastic spring. Equations of static equilibrium of the beam are represented by the static version of Eq. (3), and the boundary conditions are

$$\begin{aligned} &x = 0\text{: } w = 0, \qquad u = 0, \qquad \frac{\mathrm{d}w}{\mathrm{d}x} = -K^{-1}M \\ &x = L\text{: } M = 0, \qquad N = 0, \qquad Q = \frac{\mathrm{d}M}{\mathrm{d}x} = P \end{aligned} \tag{32}$$

If the crack is longer than the half-thickness of the beam, the condition $u(x = 0) = 0$ becomes invalid, but such a case corresponding to an extensive damage that usually results in a rapid collapse is not considered here.

The solution of the equations of equilibrium yields both the transverse and axial displacements. Applying boundary conditions to specify the constants of integration, the deflection of the free end is related to the applied force by

$$w(x = L) = \frac{PL^2}{3[D - (B^2/A)]b}\left[L + 3K^{-1}\left(D - \frac{B^2}{A}\right)b\right] \tag{33}$$

If the displacement magnification factor q is defined as a ratio of the deflection of the tip of the cantilever with a root crack to that in the intact counterpart subject to the same load, the coefficient K is determined from

$$K = \frac{3[D - (B^2/A)]b}{(q-1)L} \tag{34}$$

Therefore, using experimental data from the tests on beams with the known depth of the crack, it is possible to establish a relationship between this depth and the stiffness of the rotational constraint K. Alternatively, this stiffness can be found from finite element analysis, such as ABAQUS, employed in the Numerical Examples section.

2. Vibrations of a FGM Beam with Rotational Restraint (Open Crack)

The problem of free vibrations of the beam can be analyzed using the equations of motion (3) without the term $m\ddot{v}$ and using the boundary conditions (32) with $P = 0$. The solution is sought by representing both axial and transverse displacements in the form of Eq. (6). This solution may be further simplified by neglecting the effect of the axial inertia on both transverse and axial motions. The inaccuracy introduced by this simplification is insignificant, as follows from the comparison between analytical and finite element results (see Numerical Examples). Accordingly, the solution is presented as

$$\begin{aligned} w &= W\bar{\eta}(x)\sin\lambda t = (C_1\sinh\bar{\beta}x + C_2\cosh\bar{\beta}x + C_3\sin\bar{\beta}x \\ &\quad + C_4\cos\bar{\beta}x)\sin\lambda t \\ u &= W\bar{\varphi}(x)\sin\lambda t = \frac{B}{A}\frac{\mathrm{d}w}{\mathrm{d}x} + C_5\sin\lambda t \end{aligned} \tag{35}$$

where C_j are constants of integration; $\bar{\beta}$ is given by Eq. (7b), omitting the subscript n; and the boundary condition $N(x = L) = 0$ is already accounted for.

The application of the boundary conditions yields the following system of equations:

$$\begin{bmatrix} 0 & 1 & 0 & 1 \\ 1 & -K^{-1}\left[D - \frac{B^2}{A}\right]\bar{\beta} & 1 & K^{-1}\left[D - \frac{B^2}{A}\right]\bar{\beta} \\ \sinh\bar{\beta}L & \cosh\bar{\beta}L & -\sin\bar{\beta}L & -\cos\bar{\beta}L \\ \cosh\bar{\beta}L & \sinh\bar{\beta}L & -\cos\bar{\beta}L & \sin\bar{\beta}L \end{bmatrix} \times \begin{Bmatrix} C_1 \\ C_2 \\ C_3 \\ C_4 \end{Bmatrix} = 0 \tag{36}$$

and the constant of integration in the expression for axial displacements is

$$C_5 = -\frac{B}{A}\bar{\beta}(C_1 + C_3) \tag{37}$$

The natural frequencies can be determined from the requirement that the determinant of Eq. (36) should be equal to zero. Subsequently, the solution is represented by Eq. (35) and the normal modes corresponding to the ith natural frequency are given by

$$\begin{aligned} \bar{\eta}_i(x) &= \sinh\bar{\beta}_i x + f_{2i}\cosh\bar{\beta}_i x + f_{3i}\sin\bar{\beta}_i x + f_{4i}\cos\bar{\beta}_i x \\ \bar{\varphi}_i(x) &= \frac{B}{A}\bar{\beta}_i[(\cosh\bar{\beta}_i x - 1) + f_{2i}\sinh\bar{\beta}_i x + f_{3i}(\cos\bar{\beta}_i x - 1) \\ &\quad + f_{4i}\sin\bar{\beta}_i x] \end{aligned} \tag{38}$$

where $\bar{\beta}_i = \bar{\beta}_i(\lambda_i)$ and the coefficients $f_{ji} = C_j/C_1$ are found from Eqs. (36) and (37) using the ith natural frequency and $C_1 = 1$.

The forced motion of the beam is governed by the system of equations (3) and the boundary conditions:

$$\begin{aligned} &x = 0\text{: } w = v, \qquad u = 0, \qquad \frac{\mathrm{d}w}{\mathrm{d}x} = -K^{-1}M \\ &x = L\text{: } M = 0, \qquad N = 0, \qquad Q = \frac{\mathrm{d}M}{\mathrm{d}x} = 0 \end{aligned} \tag{39}$$

The displacements are sought in the form of the series in terms of normal modes:

$$w = \sum_i W_i\bar{\eta}_i(x)\sin\omega t, \qquad u = \sum_i W_i\bar{\varphi}_i(x)\sin\omega t \tag{40}$$

The amplitude of the terms in series (40) is available from the equations of motion:

$$W_i = \frac{m\omega^2\bar{g}_i V}{[(D - B^2/A)\bar{\beta}_i^4 - m\omega^2]\bar{f}_i} \tag{41}$$

where

$$\bar{g}_i = \int_0^L \bar{\eta}_i \, \mathrm{d}x, \qquad \bar{f}_i = \int_0^L \bar{\eta}_i^2 \, \mathrm{d}x \tag{42}$$

E. Vibrations of a FGM Cantilever with a Root Crack Subject to Temperature

FGM beams often operate in high-temperature environments. An example is a FGM turbine blade modeled as a nonprismatic cantilever beam of a variable cross section subject to temperature that mostly varies in the thickness direction. In addition to nonprismatic beams, the following discussion also refers to beams with a uniform cross section but variable grading in the axial direction and that are subject to thermal loads. It is noted that the effect of temperature on eigenfrequencies of structures has also been investigated by other researchers; mentioned here are papers by Librescu et al. [22,23]. Contrary to the previous studies, this section presents a qualitative conclusion regarding the frequencies of a beam exposed to an arbitrary thermal environment.

If a nonprismatic FGM beam is subject to an arbitrary temperature distribution, the constitutive relations are modified to account for variable stiffness and thermal terms:

$$\begin{aligned} N &= \bar{A}(\hat{T},x)\frac{\partial u}{\partial x} - \bar{B}(\hat{T},x)\frac{\partial^2 w}{\partial x^2} - N^T(\hat{T},x) \\ M &= \bar{B}(\hat{T},x)\frac{\partial u}{\partial x} - \bar{D}(\hat{T},x)\frac{\partial^2 w}{\partial x^2} - M^T(\hat{T},x) \end{aligned} \tag{43}$$

where $\hat{T}$ is the temperature (the heat conduction problem is assumed to be solved), and

$$\begin{aligned} &\{N^T(\hat{T},x), M^T(\hat{T},x)\} \\ &\quad = \int_y \int_z Q_{11}(\hat{T},x,z)\alpha(\hat{T},x,z)\hat{T}(x,y,z)\{1,z\}\,\mathrm{d}z\,\mathrm{d}y \end{aligned} \tag{44}$$

It is emphasized that the terms N and M in Eq. (43) represent the force and moment, rather than the stress resultant and stress couple. In the case of a nonprismatic beam, the stiffness terms in Eq. (44) are

$$\{\bar{A}(\hat{T},x), \bar{B}(\hat{T},x), \bar{D}(\hat{T},x)\} = \int_y \int_z Q_{11}(\hat{T},x,z)\{1,z,z^2\}\,\mathrm{d}z\,\mathrm{d}y \tag{45}$$

The reduced stiffness $Q_{11}(\hat{T},x,z)$ and the coefficient of thermal expansion $\alpha(\hat{T},x,z)$ reflect the influence of external thermal load that affects the distribution of temperature throughout the beam and, accordingly, the properties of the material.

The equations of free vibrations of the beam are written to include the effect of in-plane force:

$$N_{,x} = m(x)\ddot{u} \tag{46a}$$

$$M_{,xx} + (Nw_{,x})_{,x} = m(x)\ddot{w} \tag{46b}$$

where

$$m(x) = \int_y \int_z \rho \, \mathrm{d}z \, \mathrm{d}y$$

is a mass per unit length that varies in the x direction.

The response of the beam is now subdivided into static and dynamic components so that

$$u = u^0 + \tilde{u}, \qquad w = w^0 + \tilde{w} \tag{47}$$

Equations of motion obtained by the substitution of Eqs. (43) and (47) into Eq. (46) become

$$\begin{aligned} &\frac{\partial}{\partial x}\left[\bar{A}(\hat{T},x)\left(\frac{\partial u^0}{\partial x} + \frac{\partial \tilde{u}}{\partial x}\right)\right] - \frac{\partial}{\partial x}\left[\bar{B}(\hat{T},x)\left(\frac{\partial^2 w^0}{\partial x^2} + \frac{\partial^2 \tilde{w}}{\partial x^2}\right)\right] \\ &\quad - \frac{\partial N^T(\hat{T},x)}{\partial x} - m(x)\ddot{\tilde{u}} = 0 \\ &\frac{\partial^2}{\partial x^2}\left[\bar{B}(\hat{T},x)\left(\frac{\partial u^0}{\partial x} + \frac{\partial \tilde{u}}{\partial x}\right) - \bar{D}(\hat{T},x)\left(\frac{\partial^2 w^0}{\partial x^2} + \frac{\partial^2 \tilde{w}}{\partial x^2}\right) - M^T(\hat{T},x)\right] \\ &\quad - \frac{\partial[N^0(w^0+\tilde{w})_{,x}]}{\partial x} - \frac{\partial}{\partial x}[(\bar{A}(\hat{T},x)\tilde{u}_{,x} - B(\hat{T},x)\tilde{w}_{,xx}) \\ &\quad \times (w^0+\tilde{w})_{,x}] - m(x)\ddot{\tilde{w}} = 0 \end{aligned} \tag{48}$$

where N^0 is the static axial force that is equal to zero. This is evident when considering the static version of Eq. (46a), which implies that this force is constant and the boundary condition $N(x=L)=0$.

Retaining linear dynamic terms in Eq. (48) yields the system of equations:

$$\frac{\partial}{\partial x}\left[\bar{A}(\hat{T},x)\frac{\partial \tilde{u}}{\partial x}\right] - \frac{\partial}{\partial x}\left[\bar{B}(\hat{T},x)\frac{\partial^2 \tilde{w}}{\partial x^2}\right] - m(x)\ddot{\tilde{u}} = 0 \tag{49a}$$

$$\begin{aligned} &\frac{\partial^2}{\partial x^2}\left[\bar{B}(\hat{T},x)\frac{\partial \tilde{u}}{\partial x} - \bar{D}(\hat{T},x)\frac{\partial^2 \tilde{w}}{\partial x^2}\right] \\ &\quad \underline{- \frac{\partial}{\partial x}[(\bar{A}(\hat{T},x)\tilde{u}_{,x} - B(\hat{T},x)\tilde{w}_{,xx})w^0{}_{,x}]} - m(x)\ddot{\tilde{w}} = 0 \end{aligned} \tag{49b}$$

It is obvious from Eq. (49) that static deflections due to thermal loading affect equations of motion and, accordingly, the eigenvalues. This effect is introduced through the underlined term in Eq. (49b).

Dynamic boundary conditions obtained from the correspondingly modified Eqs. (32) are uncoupled from the corresponding static conditions:

$$\begin{aligned} &x=0\text{: } \tilde{w} = \tilde{u} = 0, \qquad \frac{\mathrm{d}\tilde{w}}{\mathrm{d}x} = -K^{-1}\left[\bar{B}(\hat{T},x)\frac{\partial \tilde{u}}{\partial x} - \bar{D}(\hat{T},x)\frac{\partial^2 \tilde{w}}{\partial x^2}\right] \\ &x=L\text{: } \tilde{N} = \bar{A}(\hat{T},x)\frac{\partial \tilde{u}}{\partial x} - \bar{B}(\hat{T},x)\frac{\partial^2 \tilde{w}}{\partial x^2} = 0 \\ &\tilde{M} = \bar{B}(\hat{T},x)\frac{\partial \tilde{u}}{\partial x} - \bar{D}(\hat{T},x)\frac{\partial^2 \tilde{w}}{\partial x^2} = 0, \qquad \tilde{Q} = \frac{\mathrm{d}\tilde{M}}{\mathrm{d}x} = 0 \end{aligned} \tag{50}$$

The last condition in Eq. (50) accounts for the fact that both static and dynamic axial forces at the free end are equal to zero.

The equations of motion are affected by thermal terms, even if the temperature is uniform. Therefore, the frequencies of vibrations, including the fundamental frequency, and the corresponding eigenvectors are influenced by static thermal loading.

If the effect of the axial inertia was neglected, the first equation of motion would be reduced to $N^0{}_{,x} + \tilde{N}_{,x} = 0$. Accordingly, the boundary condition $N(x=L)=0$ implies $N^0 = \tilde{N} = 0$ and Eq. (46b) becomes

$$M_{,xx} = m(x)\ddot{w} \tag{51}$$

The equations are still temperature-dependent through the material properties, but the nonlinear term $(\partial/\partial x)(Nw_{,x})$ is now equal to zero in Eq. (51) and the associated temperature effect is not included in Eq. (49b). In conclusion, even in the case of a prismatic beam subject to temperature that is independent of the axial coordinate, the explicit effect of temperature on free vibrations is present as long as axial inertia is accounted for (in addition, temperature affects natural frequencies through its influence on material properties).

III. Numerical Examples

The following examples are based on a beam manufactured from Ti and TiB (titanium boride), because data were available for the fundamental frequency for intact specimens. The length, width, and thickness of the beam were 101.6 (unless indicated otherwise), 25.4, and 3.175 mm, respectively. All seven layers were quasi-isotropic,

Table 1 Geometry and material properties of functionally graded beams considered in examples and experiments.

Layer	Layer thickness, mm	% Ti	% TiB	E, GPa[a]	E, GPa[b]	ν^a	ν^b
7	0.9398	15	85	274	366	0.17	0.31
6	0.4064	25	75	237	328	0.19	0.295
5	0.4064	40	60	193	275	0.22	0.295
4	0.4064	55	45	159	228	0.25	0.3
3	0.4064	70	30	133	185	0.28	0.3
2	0.4064	85	15	120	148	0.31	0.21
1	0.2032	100	0	107	116	0.34	0.31

[a]Layer properties according to [24].
[b]Layer properties according to the manufacturer (Cercom, Inc.).

each layer having constant volume fractions of TiB and Ti. The composition and thickness of the layers are shown in Table 1. The same table presents the properties of each layer measured by Hall and Lin [24] and estimated by the beam manufacturer, Cercom, Inc. A side view of the beam photographed with a 50× magnification is shown in Fig. 4. The variations of the modulus of elasticity and the Poisson ratio dependent on the volume fraction of titanium boride are illustrated in Fig. 5. The examples discussed next are presented for the beam with a single crack at the root, similar to that shown in Fig. 3. The fact that this mode of damage was observed in experiments motivated close attention to the effect of a root crack on the fundamental frequency of the beam. If this is significant, it would both affect the resonant conditions and motivate using nondestructive testing when monitoring the natural frequencies.

The displacement of the tip of a cantilever beam statically loaded by a force P (Fig. 3) is shown as a function of the depth of the crack in Fig. 6. These results were generated numerically by ABAQUS to elucidate the effect of the crack on maximum displacements and were used in Eqs. (33) or (34) to evaluate the stiffness of the equivalent rotational spring. The beam model used in ABAQUS used four-noded shell elements. Each layer was modeled with the mechanical properties from Table 1. The crack was modeled by removing constraints against displacements at the corresponding nodes of the elements adjacent to the boundary of the beam. As follows from Fig. 6, the effect of the crack becomes noticeable as its depth approaches 1 mm (i.e., about a third of the depth of the beam). Predictably, this effect is particularly prominent for cracks originating at the stiffer titanium boride surface.

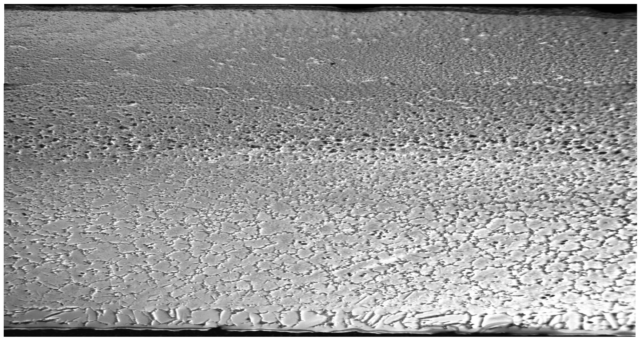

Fig. 4 Photograph of a TiB/Ti FGM beam magnified by a factor of 50.

The spring constant is shown as a function of the displacement magnification factor in Fig. 7, in which the latter factor is kept in the range anticipated based on the previous analysis (Fig. 6). The stiffness becomes infinite for the magnification factor equal to zero, because this corresponds to the intact beam with a complete clamping. However, as follows from Fig. 7, the stiffness rapidly decreases, even as a result of relatively short cracks.

The effect of the stiffness of the rotational spring on the fundamental frequency is shown in Fig. 8, in which the nondimensional compliance $k = K^{-1}(D - B^2/A)$. The nondimensional stiffness varies in the range anticipated for cracks considered in examples that do not exceed a half-thickness of the beam. It is evident that the changes in the fundamental frequency as a result of the root crack are large enough to justify vibrational nondestructive testing. The presence of a crack also affects the resonant conditions for the structure. This means that a beam that did not develop large vibrations under a load with the prescribed frequency may exhibit violent response as its fundamental frequency decreases due to a root crack. The result shown in Fig. 9 elucidates the effect of the length of the beam with a root crack on its fundamental frequencies. Although numerical results depend on the length of the beam, the qualitative conclusions remain unaltered.

Finally, fundamental frequencies of a FGM cantilever beam are shown as functions of the depth of the root crack in Fig. 10. It is seen

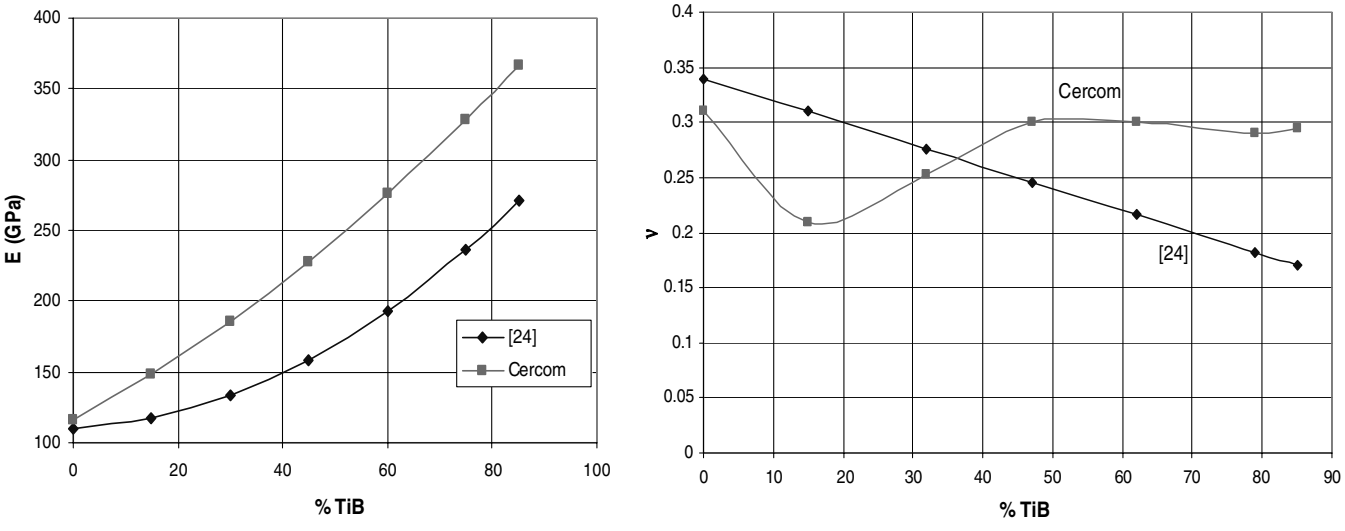

Fig. 5 Variations of the modulus of elasticity (left) and the Poisson ratio (right) as functions of the volume fraction of titanium boride.

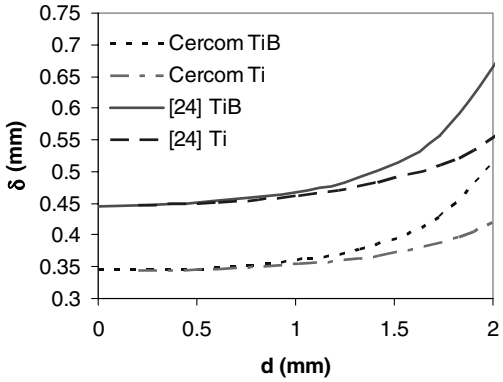

Fig. 6 Displacement of the tip of FGM beam δ as a function of crack depth from ABAQUS; TiB denotes the crack initiated at the TiB-rich surface and Ti denotes the crack initiated at the titanium surface.

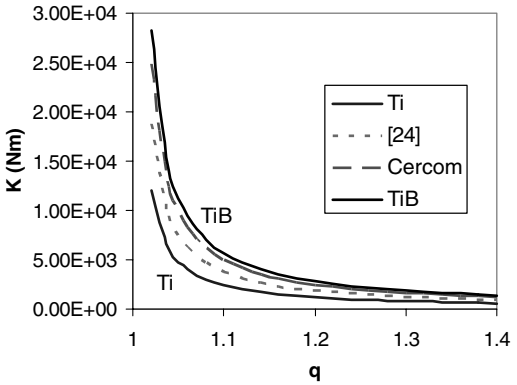

Fig. 7 Stiffness of the rotational spring as a function of the displacement magnification factor; Ti denotes the purely titanium beam, TiB denotes the beam consisting of 85% TiB and 15% Ti, [25] denotes the FGM beam with properties according to [24], and Cercom denotes the FGM beam with properties according to Cercom, Inc.

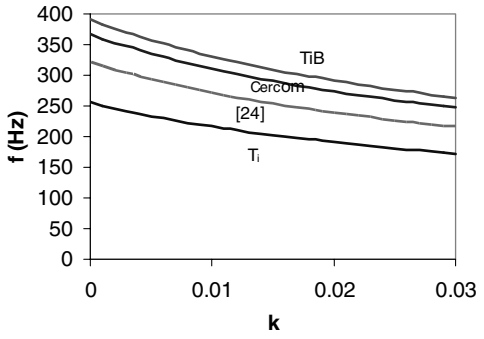

Fig. 8 Fundamental frequency as a function of the nondimensional compliance of the FGM beam; Ti denotes the purely titanium beam, TiB denotes the beam consisting of 85% TiB and 15% Ti, [25] denotes the FGM beam with properties according to [24], and Cercom dentoes the FGM beam with properties according to Cercom, Inc.

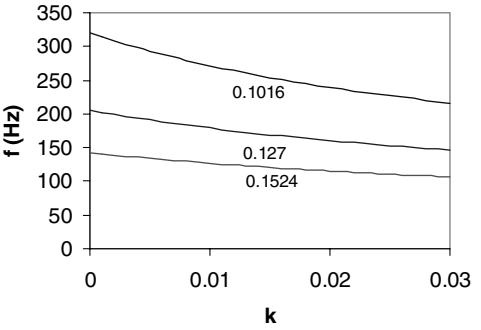

Fig. 9 Effect of the length of a FGM beam with a root crack on the fundamental frequency; labels represent the length of the beam in meters; and material properties are according to [24].

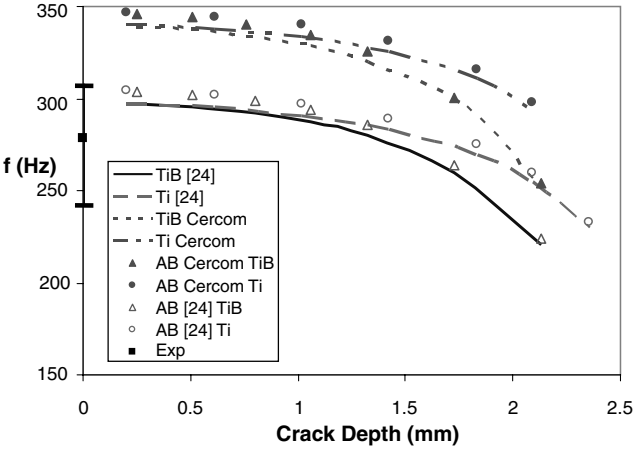

Fig. 10 The fundamental frequency of a FGM cantilever beam as a function of the depth of the crack at the clamped end; TiB denotes the crack initiated at the TiB-rich surface, Ti denotes the crack initiated at the titanium surface, solid curves denote the results of the analytical solution, AB denotes the ABAQUS results, and Exp denotes the experimental result.

that the analytical solution that neglected the axial inertia agrees well with the results obtained by ABAQUS, which accounted for this inertia. It is obvious from Fig. 10 that cracks deeper than 1 mm noticeably affect the fundamental frequency of the beam. Predictably, cracks originating from the stiffer surface resulted in a larger reduction in the fundamental frequency than identical cracks that started at the surface on which the stiffness is lower.

A comparison with data from intact beams indicates that the prediction of the layerwise beam properties provided in [24] yields a better accuracy than the alternative set from Cercom, Inc. In these tests, the beams were clamped in a fixture and tapped with an instrumented hammer. An accelerometer was used to measure the beam response and the signal was analyzed for the fundamental frequency. The effect of the mass of the accelerometer was estimated using the Dunkerley method [25]. Using the analytical solution and properties from [24], the fundamental frequency for the intact FGM beam is about 6% higher than the average of the test results. The error bars show the range of the experimentally measured frequencies. As can be seen, the scatter in the data is large ($\approx \pm$ 12%) and may be an indication of microcracking in the material or this may be an indication of the variability of the material properties associated with the method of manufacture of the specimens. Tests with uniform material (aluminum and uniform 85%TiB/15%Ti specimens) showed less scatter ($\approx \pm$ 1%) and agreed well with theory. In any case, a decrease of frequency would be expected once a crack occurs.

It is emphasized that the results shown in Figs. 8–10 were obtained by assuming that the crack remains open and unaffected by the presence of the boundary throughout the cycle of motion. Accordingly, these results represent the lower limit of the fundamental frequency. The upper limit can easily be evaluated from Fig. 10 as $f_u(d) = 2/[f^{-1}(d) + f^{-1}(d = 0)]$. As anticipated, the difference between the lower and upper limits remains small if the crack is short. For example, for a 1-mm-deep crack that initiated at the TiB-rich surface of the beam, this difference is only 2.5% (using the properties from [24]). However, if the crack is 2 mm deep, this difference exceeds 13%. Nevertheless, it should be emphasized that such deep cracks exceeding 60% of the thickness of the beam are

unlikely to be encountered in applications. Therefore, the lower limit of the frequency remains a valid estimate that is also conservative in numerous applications in which driving frequencies are lower than the fundamental frequency of the structure.

IV. Conclusions

The paper presents the analysis of free and forced vibrations of a damaged cantilever FGM beam. The modes of damage considered in this paper include a region with degraded stiffness, delamination, and root cracks. The solutions of free-vibration problems are exact, whereas forced vibrations are determined by the mode-summation method. Numerical results elucidate the effect of root cracks on the fundamental frequency of a FGM beam. As follows from these examples, changes in the fundamental frequency due to the presence of a root crack are sufficiently large to warrant using a nondestructive vibration test for detection of such damage. At the same time, the fact that natural frequencies noticeably decrease as a result of a root crack implies that FGM beams designed for a certain range of frequencies may degrade into a resonant frequency range as a result of local damage.

A qualitative analysis of the effect of static thermal loading on free vibrations of a FGM cantilever beam with the stiffness varying in the axial direction and a root crack is also conducted. The variation of the stiffness can occur if the beam is nonprismatic or if material grading is a function of the axial coordinate. It is shown that static thermal loading affects free vibrations (including fundamental frequencies) of a FGM beam, even if the problem is geometrically linear. However, nonlinear effects will be missed if axial inertia is excluded from the analysis. The same observation remains valid for uniform FGM beams, even if temperature is independent of the axial coordinate.

An interesting observation made during experimental testing of FGM specimens used to validate the theory refers to a significant scatter of the modulus of elasticity and the Poisson ratio of FGM components with quasi-isotropic layers. Such scatter was present even though the specimen fabrication was closely monitored. This observation should serve as a warning to designers considering FGM to always validate material properties before their use in structural applications. The scatter of properties may also justify using statistical methods to characterize the behavior of FGM structures.

Appendix: Effect of the Axial Inertia on the Fundamental Frequency of a Composite Beam

The equations of motion of a slender asymmetrically laminated or FGM beam are

$$A\frac{\partial u^2}{\partial x^2} - B\frac{\partial^3 w}{\partial x^3} - m\ddot{u} = 0, \qquad B\frac{\partial^3 u}{\partial x^3} - D\frac{\partial^4 w}{\partial x^4} - m\ddot{w} = 0 \quad \text{(A1)}$$

The boundary conditions corresponding to simply supported edges that are not constrained against axial displacements are satisfied if

$$u = U\cos\frac{\pi x}{L}e^{i\lambda t}, \qquad w = W\sin\frac{\pi x}{L}e^{i\lambda t} \quad \text{(A2)}$$

where the amplitudes of axial and transverse vibrations are denoted by U and W, respectively.

The substitution of Eq. (A2) into Eq. (A1) and straightforward transformations yield

$$\lambda^2 = \frac{[D - (B^2/A)](\pi/L)^4}{m[1 - (B/A)(\pi/L)(U/W)]} \quad \text{(A3)}$$

The ratio of the fundamental frequency obtained by accounting for the effect of the axial inertia compared with the ratio without this effect is now evaluated as

$$r = \sqrt{\frac{1}{[1 + (B/A)(\pi/L)(U/W)]}} \approx 1 - \frac{1}{2}\frac{B}{A}\frac{\pi}{L}\frac{U}{W} \quad \text{(A4)}$$

For a beam analyzed in numerical examples, $A = 6.621\times 10^8$ N/m, $B = 2.818 \times 10^5$ N, and $L = 0.1016$ m, where the stiffness coefficients are obtained using the properties suggested in [24]. Accordingly, Eq. (A4) yields $r = 1 - 0.00658(U/W)$. Considering the fact that the amplitude of axial vibrations represents only a small fraction of the transverse amplitude, it is obvious that the effect of the axial inertia on the fundamental frequency is negligible. The same conclusion can be reached by considering other typical composite and FGM beam configurations and using the estimate given by (A4).

Acknowledgment

This research was sponsored by the Structural Sciences Center, Air Vehicles Directorate of the U.S. Air Force Research Laboratory through contract GS-23F8049H (F33601-03-F-0060).

References

[1] Suresh, S., and Mortensen, A., *Fundamentals of Functionally Graded Materials*, IOM Communications, London, 1998.

[2] Miyamoto, Y., Kaysser, W. A., Rabin, B. H., Kawasaki, A., and Ford, R. G., *Functionally Graded Materials: Design, Processing and Applications*, Kluwer Academic, Dordrecht, 1999.

[3] Paulino, G. H., Jin, Z. H., and Dodds, R. H., Jr., "Failure of Functionally Graded Materials," *Comprehensive Structural Integrity*, edited by B. Karihallo, and W. G. Knauss, Vol. 2, Elsevier Science, New York, 2003, Chap. 13, pp. 607–644.

[4] Noda, N., "Thermal Stresses in Functionally Graded Material," *Journal of Thermal Stresses*, Vol. 22, Nos. 4–5, 1999, pp. 477–512.

[5] Sankar, B. V., "An Elasticity Solution for Functionally Graded Beams," *Composites Science and Technology*, Vol. 61, No. 5, 2001, pp. 689–696.

[6] Chakraborty, A., Gopalakrishnan, S., and Reddy, J. N., "A New Beam Finite Element for the Analysis of Functionally Graded Materials," *International Journal of Mechanical Sciences*, Vol. 45, No. 3, 2003, pp. 519–539.

[7] Chakraborty, A., and Gopalakrishnan, S., "A Spectrally Formulated Finite Element for Wave Propagation Analysis in Functionally Graded Beams," *International Journal of Solids and Structures*, Vol. 40, No. 10, 2003, pp. 2421–2448.

[8] Hudnut, S., Almajid, A., and Taya, M., "Functionally Graded Piezoelectric Bimorph-Type Actuator," *Smart Structures and Materials 2000*, Proceedings of SPIE–the International Society for Optical Engineering, Vol. 3992, 2003, pp. 376–386.

[9] Alexander, P. W., and Brei, D., "The Design Tradeoffs of Linear Functionally Graded Piezoceramic Actuators," 2003 ASME International Mechanical Engineering Congress and Exposition, American Society of Mechanical Engineers Paper 2003-42723, 2003.

[10] Takagi, K., Li, J.-F., Yokogama, S., and Watanabe, R., "Fabrication and Evaluation of PZT/Pt Piezoelectric Composites and Functionally Graded Actuators," *Journal of the European Ceramic Society*, Vol. 23, No. 10, 2003, pp. 1577–1583.

[11] Li, J.-F., Takagi, K., Ono, M., Pan, W., Watanabe, R., Almajid, A., and Taya, M., "Fabrication and Evaluation of Porous Piezoelectric Ceramics and Porosity-Graded Actuators," *Journal of the American Ceramic Society*, Vol. 86, No. 7, 2003, pp. 1094–1098.

[12] Alexander, P. W., Brei, D., and Halloran, J. W., "DEPP Co-Extruded Functionally Graded Piezoceramics," 2005 ASME International Mechanical Engineering Congress and Exposition, American Society of Mechanical Engineers Paper 2005-80217, 2005.

[13] Noor, A. K., "Finite Element Buckling and Postbuckling Analyses," *Buckling and Postbuckling of Composite Plates*, edited by G. J. Turvey, and I. H. Marshall, Chapman & Hall, London, 1995, pp. 58–107.

[14] Whitney, J. M., *Structural Analysis of Laminated Anisotropic Plates*, Technomic, Lancaster, PA, 1987.

[15] Reddy, J. N., *Mechanics of Laminated Composite Plates and Shells. Theory and Analysis*, 2nd ed., CRC Press, Boca Raton, FL, 2004.

[16] Bert, C. W., and Gordaninejad, F., "Transverse Shear Effects in Bimodular Composite Laminates," *Journal of Composite Materials*, Vol. 17, No. 4, 1983, pp. 282–298.

[17] Dorf, R. C., *Modern Control Systems*, 5th ed., Addison–Wesley, Reading, MA, 1989.

[18] Luo, H., and Hanagud, S., "Dynamics of Delaminated Beams," *International Journal of Solids and Structures*, Vol. 37, No. 10, 2000, pp. 1501–1519.
[19] Wang, J., and Tong, L., "A Study of the Vibration of Delaminated Beams Using a Nonlinear Anti-Interpenetration Constraint Model," *Composite Structures*, Vol. 57, No. 1, 2002, pp. 483–488.
[20] Yin, W. L., and Jane, K. C., "Vibration of a Delaminated Beam-Plate Relative to Buckled States," *Journal of Sound and Vibration*, Vol. 156, No. 1, 1992, pp. 125–140.
[21] Simitses, G. J., "Delamination Buckling of Flat Laminates," *Buckling and Postbuckling of Composite Plates*, edited by G. J. Turvey, and I. H. Marshall, Chapman & Hall, London, 1995, pp. 299–328.
[22] Librescu, L., and Lin, W., "Vibration of Thermomechanically Loaded Flat and Curved Panels Taking into Account Geometric Imperfections and Tangential Edge Restraints," *International Journal of Solids and Structures*, Vol. 34, No. 17, 1997, pp. 2161–2181.
[23] Librescu, L., Lin, W., Nemeth, M. P., and Starnes, J. H., Jr., "Vibration of Geometrically Imperfect Panels Subjected to Thermal and Mechanical Loads," *Journal of Spacecraft and Rockets*, Vol. 33, No. 2, 1996, pp. 285–291.
[24] Hill, M. R., and Lin, W.-Y., "Residual Stress Measurement in a Ceramic-Metallic Graded Material," *Journal of Engineering Materials and Technology*, Vol. 124, No. 2, 2002, pp. 185–191.
[25] Rao, S. S., *Mechanical Vibrations*, 3rd ed., Addison–Wesley, Reading, MA, 1995.

A. Palazotto
Associate Editor